RSC Advances

PAPER

View Article Online
View Journal | View Issue

Cite this: *RSC Adv.*, 2025, **15**, 27924

Highly phase-separated alternating copolymer of alkyl vinyl ether and sulfonic acid group-containing trifluoro vinyl ether

Kaishi Hori, [a] Shoji Miyanishi [b] and Takeo Yamaguchi *[b]

This study explores the development of novel cation exchange membranes (CEMs) by synthesizing alternating copolymers of perfluorosulfonic acid monomers and alkyl vinyl ethers with varying chain lengths. Unlike traditional Nafion-based CEMs, which form cluster-channel morphologies, the newly synthesized copolymers exhibit well-defined lamellar structures. Small-angle X-ray scattering (SAXS) and transmission electron microscopy (TEM) analyses revealed that increasing the alkyl chain length enhances the area of these structures. Moreover, self-diffusion coefficient measurements by PFG-NMR showed that water diffusivity increased with longer side chains, despite a decrease in ion exchange capacity (IEC). This inverse relationship highlights the importance of morphological control in optimizing membrane transport properties. The findings demonstrate that integrating hydrocarbon and fluorocarbon components enables the design of distinct phase-separated structures, expanding the landscape of structure–property relationships in ion-conducting materials. These insights offer new strategies for engineering high-performance membranes for energy and water-related applications.

Received 20th June 2025
Accepted 31st July 2025

DOI: 10.1039/d5ra04403k

rsc.li/rsc-advances

Introduction

Cation exchange membranes (CEMs) are crucial in various applications, including food production, water purification, energy generation, and energy storage. The ability to selectively transport cations and neutral molecules is key to their utility in this field. The transport capacity and selectivity of the ions and neutral molecules depend on the higher-order structure of the ion exchange membranes. Consequently, precise control of this higher-order structure through design and film formation processes is imperative.[1–6]

The polymeric materials used in CEMs can be categorized into two distinct classes: hydrocarbons and perfluorinated polymers. Hydrocarbon polymers include various structures such as sulfonated poly(ether ether ketone), sulfonated poly(ether sulfone), and sulfonated polybenzimidazole. Their structural design flexibility allows the formation of diverse higher-order structures, including cylinders, lamellae, and gyroid (Fig. 1, top).[7–9]

In contrast, perfluorosulfonic acid (PFSA), a copolymer of tetrafluoroethylene and a perfluorosulfonic acid monomer, is a prime example of a perfluorinated polymer (Fig. 1, bottom). The PFSA chain uniquely combines a hydrophobic poly(tetrafluoroethylene) moiety and a hydrophilic sulfonic acid moiety. This combination results in a microphase-separated structure. Specifically, the sulfonic acid groups of the hydrophilic moiety aggregate to form clusters, which are connected *via* narrow channels to form a continuous network.[10–12] This microphase-separated structure functions as a proton transport pathway, significantly contributing to the ionic conductivity of the membrane.

In PFSA, the cluster size and network structure can be controlled by modifying the side chain, copolymerization ratio, film formation, and alkali treatment conditions.[13–15] However, fundamentally modifying the phase-separation morphology, such as the continuity and shape of the structure, using these methods remains challenging. Consequently, the development of novel molecular designs is imperative to explore a more diverse array of phase-separation structures.

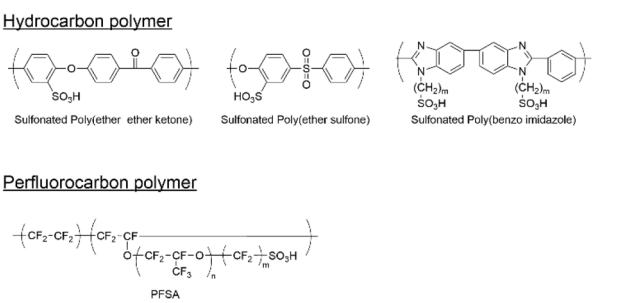

Fig. 1 Typical structures of hydrocarbon and perfluorocarbon polymers in CEMs.

[a]*Research Laboratory of Advanced Science & Technology, Corporate Research & Development, Asahi Kasei Corporation, 2-1 Samejima, Fuji, Shizuoka, 416-8501, Japan*
[b]*Laboratory for Chemistry, Life Science Institute of Innovative Research, Science Tokyo, R1-17, 4259, Midori-ku, Yokohama, Kanagawa, 226-8503, Japan. E-mail: yamag@res.titech.ac.jp*

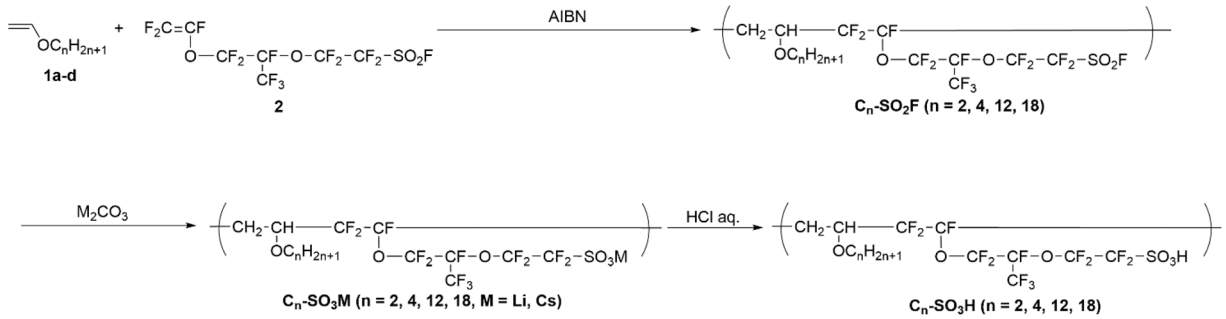

Scheme 1 Synthesis scheme for an alkyl vinyl ether-perfluorosulfonic acid monomer copolymer.

A review of the existing literature reveals that most research on CEMs has focused on hydrocarbon-based polymers and PFSA. However, studies on structures with hydrocarbon and fluorocarbon backbones coexisting are scarce.[16–19] Notably, to date, no research has specifically investigated the phase-separated structures resulting from the copolymerization of perfluorosulfonic acid and hydrocarbon monomers. As previously highlighted, the phase-separated structure directly influences the mass-transport properties. Therefore, the copolymers of perfluorosulfonic acid monomers with hydrocarbon monomers of various structures can induce a phase-separated structure that is different from PFSA. This could advance our understanding of the structure–property relationships.

Controlling the polymerization sequence is one of the most effective methods for controlling the morphology of polymer materials. Block copolymerization allows the morphology to be tuned by changing the block length and monomer ratio, but it requires multi-step polymerization reactions or precise polymerization conditions.[20,21] On the other hand, alternating copolymers can be polymerized in a single step and do not require particularly precise polymerization conditions. Chen *et al.* reported that perfluorosulfonic acid monomers and vinyl ether compounds form well defined alternating copolymers through radical polymerization using organic catalysts.[22]

In this study, we focused on the perfluorosulfonic acid monomer (the monomer unit of PFSA) and examined the structural outcomes when it was copolymerized with various hydrocarbon monomers. We selected vinyl ethers as comonomers because of their donor–acceptor alternating copolymerization with electron-accepting fluoro olefins. Then we synthesized alternating copolymers by reacting a perfluorosulfonic acid monomer with alkyl vinyl ethers of different chain lengths (Scheme 1). The resulting copolymers were analyzed using small-angle X-ray scattering (SAXS) and transmission electron microscopy (TEM) to understand the morphology differences driven by their distinct chemical structures.

Experimental

General

HFC43-10mee was purchased from Chemours™. Water was obtained from a Merck Millipore Corp. Elix Essential UV10 water system. Perfluoro(4-methyl-3,6-dioxaoct-7-ene)sulfonyl fluoride (**2**) was prepared as described in the literature.[23,24] All other reagents were purchased from Sigma–Aldrich, Kanto Chemical, Tokyo Chemical Industries, and FUJIFILM Wako Pure Chemical Corp. and used without further purification.

The ^{1}H and ^{19}F NMR spectra were recorded on a Bruker Biospin Avance III system (400 MHz). The number-average (M_n) and weight-average (M_w) of the polymers were determined by SEC-MALS measurements using an HLC-8320GPC (Tosoh) connected to a DAWN HELEOS II MALS detector (Wyatt Technology Co.).

Elemental analysis

The C and H contents were measured using a JM10 (J-Science). F and S contents were determined using an HSU-20 (Yanako) connected with an ICS-1100 (Thermo Fisher Scientific).

The theoretical values were calculated using the following formula:

$$\text{Calcd\% X} = \sum_i (\%\ \text{monomer}_i \times M_{\text{X,monomer}_i}) \Big/ \sum_i (\%\ \text{monomer}_i \times M_{\text{monomer}_i}),$$

where calcd% X is the theoretical value of the element X content, % monomer$_i$ is the molar fraction of the monomer$_i$ in the polymer and $M_{\text{X,monomer}_i}$ and M_{monomer_i} are respectively the molecular weights of the element X in monomer$_i$ and of the monomer$_i$.

Titration measurements of the ion-exchange capacity of the polymers

The IEC values of the polymers were determined *via* titration. The polymer was first dissolved in water. The amount of acid in the solution was then measured by titrating a 0.01 N NaOH aqueous solution with an auto titrator (COM-1700, Hitachi High-Tech Corp.).

SAXS measurement

SAXS measurement was performed using a Nano-Viewer (Rigaku Holdings Corp.) at a wavelength $\lambda = 0.154$ nm. The scattering vector "q" was defined as $q = 4\pi \sin\theta/\lambda$, where 2θ is the scattering angle and λ is the wavelength of the X-ray source. The Bragg spacing "d" is related to "q" as $d = 2\pi/q$. The polymer

samples were prepared by crushing some grains into a fine powder and filling a capillary tube.

TEM image observation

The TEM image was taken using a JEM-F200 (JEOL Ltd). The ultrathin section for observation was prepared by the ultramicrotome method.

PFG-NMR measurement

^{1}H PFG-NMR spectra were recorded using a JMN-ECZL500 (JEOL Ltd). The polyelectrolyte samples (H^+) were pretreated in air at 84% relative humidity overnight in a vessel. The entire procedure, including sample packing into sealed NMR tubes, was conducted in a glovebox.

Synthesis

Copolymer of perfluoro(4-methyl-3,6-dioxaoct-7-ene)sulfonyl fluoride and ethyl vinyl ether (C_2-SO_2F). In a 100 mL two-necked round-bottom flask, 2,2′-azobis(isobutyronitrile) (73.62 mg, 0.45 mmol), perfluoro(4-methyl-3,6-dioxaoct-7-ene)sulfonyl fluoride **2** (10.00 g, 22.42 mmol), ethyl vinyl ether **1a** (4.76 g, 22.42 mmol), and 2*H*,3*H*-decafluoropentane (20.00 g) were placed under a nitrogen atmosphere. The reaction mixture was then heated to 65 °C and stirred for 24 h before cooling to room temperature. The mixture was poured into vigorously stirred MeOH (500 mL), and the MeOH was removed by decantation. The residual solid was washed three times with MeOH and dried under vacuum. The copolymer **C_2-SO_2F** was obtained in 55% yield. The sample for the NMR measurement was prepared by dissolving **C_2-SO_2F** in C_6F_6. The polymer solution was then introduced into an NMR tube along with a sealed capillary filled with $CDCl_3$ for signal lock.

^{1}H-NMR ($CDCl_3$, 400 MHz): δ 4.80–2.20 (br, 5H), δ 1.70–0.90 (br, 3H). ^{19}F NMR ($CDCl_3$, 375 MHz): δ 43.5 (s, 1F), −73.5 to 89.0 (br, 7F), −107.0 to 137.0 (br, 5F), −143.0 to 149.0 (br, 1F).

Copolymer of perfluoro(4-methyl-3,6-dioxaoct-7-ene)sulfonyl fluoride and butyl vinyl ether (C_4-SO_2F). To synthesize the copolymer **C_4-SO_2F**, a procedure similar to that used for **C_2-SO_2F** was applied. **C_4-SO_2F** was obtained from butyl vinyl ether **1b** (22.42 mmol) and **2** (22.42 mmol) with a 93% yield. The sample for the NMR measurement was prepared by dissolving **C_4-SO_2F** in C_6F_6 and introducing the polymer solution and a sealed capillary filled with $CDCl_3$ (for signal lock) into the NMR tube.

^{1}H-NMR ($CDCl_3$, 400 MHz): δ 5.00–2.20 (br, 5H), 2.20–1.20 (br, 4H), 1.10–0.60 (br, 3H). ^{19}F NMR ($CDCl_3$, 375 MHz): δ 43.1 (s, 1F), −71.0 to 89.0 (br, 7F), −106.0 to 136.0 (br, 5F), −143.8 to 147.2 (br, 1F).

Copolymer of perfluoro(4-methyl-3,6-dioxaoct-7-ene)sulfonyl fluoride and dodecyl vinyl ether (C_{12}-SO_2F). To synthesize the copolymer **C_{12}-SO_2F**, a procedure similar to that used for **C_2-SO_2F** was applied. **C_{12}-SO_2F** was obtained from dodecyl vinyl ether **1c** (22.42 mmol) and **2** (22.42 mmol) with a 71% yield.

^{1}H-NMR ($CDCl_3$, 400 MHz): δ 5.00–2.10 (br, 5H), δ 2.00–1.00 (br, 20H), 0.90 (t, 3H, J = 7.2 Hz). ^{19}F NMR ($CDCl_3$, 375 MHz): δ 45.2(s, 1F), −73.0 to 88.0 (br, 7F), −106.0 to 135.0 (br, 5F), −142.0 to 147.0 (br, 1F).

Copolymer of perfluoro(4-methyl-3,6-dioxaoct-7-ene)sulfonyl fluoride and octadecyl vinyl ether (C_{18}-SO_2F). To synthesize the copolymer **C_{18}-SO_2F**, a procedure similar to that used for **C_2-SO_2F** was applied. **C_{18}-SO_2F** was obtained from octadecyl vinyl ether **1d** (22.42 mmol) and **2** (22.42 mmol) with a 70% yield.

^{1}H-NMR ($CDCl_3$, 400 MHz): δ 5.20–2.00 (br, 5H), 1.80–1.00 (br, 32H), 0.90 (t, 3H, J = 7.2 Hz). ^{19}F NMR ($CDCl_3$, 375 MHz): δ 45.3 (s, 1F), −73.0 to 88.0 (br, 7F), −108.0 to 138.0 (br, 5F), −142.0 to 147.0 (br, 1F).

Copolymer of lithium perfluoro(4-methyl-3,6-dioxaoct-7-ene) sulfonate and ethyl vinyl ether (C_2-SO_3Li). **C_2-SO_2F** (9.59 g), Li_2CO_3 (13.70 g, 185.41 mmol), and MeOH (200 mL) were placed in a 500 mL two-necked round-bottom flask under a nitrogen atmosphere. The reaction mixture was heated to 65 °C, stirred for 48 h, and then cooled to room temperature. The mixture was filtered to remove NaF and unreacted Li_2CO_3. After filtration, the solvent was removed under reduced pressure. **C_2-SO_3Li** was obtained with a 95% yield.

^{1}H-NMR (DMSO-d_6, 400 MHz): δ 5.20–1.90 (br, 5H), δ 1.70–0.60 (br, 3H). ^{19}F NMR (DMSO-d_6, 375 MHz): δ −73.0 to 88.0 (br, 7F), −107.0 to 137.0 (br, 5F), −142.0 to 148.0 (br, 1F).

Copolymer of lithium perfluoro(4-methyl-3,6-dioxaoct-7-ene) sulfonate and butyl vinyl ether (C_4-SO_3Li). To synthesize the copolymer **C_4-SO_3Li**, a procedure similar to that used for **C_2-SO_3Li** was applied. **C_4-SO_3Li** was obtained from **C_4-SO_2F** (17.28 g) and Li_2CO_3 (23.40 g, 316.69 mmol) with a 93% yield.

^{1}H-NMR (DMSO-d_6, 400 MHz): δ 4.50–2.00 (br, 5H), 2.00–1.10 (br, 4H), 1.00–0.50 (br, 3H). ^{19}F NMR (DMSO-d_6, 375 MHz): δ −71.0 to 89.0 (br, 7F), −106.0 to 136.0 (br, 5F), −143.8 to 147.2 (br, 1F).

Copolymer of lithium perfluoro(4-methyl-3,6-dioxaoct-7-ene) sulfonate and dodecyl vinyl ether (C_{12}-SO_3Li). To synthesize the copolymer **C_{12}-SO_3Li**, a procedure similar to that used for **C_2-SO_3Li** was applied. **C_{12}-SO_3Li** was obtained from **C_{12}-SO_2F** (11.34 g) and Li_2CO_3 (12.73 g, 172.28 mmol) with a 91% yield.

^{1}H-NMR (DMSO-d_6, 400 MHz): δ 4.80–2.10 (br, 5H), δ 2.00–0.95 (br, 20H), 0.95–0.50 (br, 3H). ^{19}F NMR (DMSO-d_6, 375 MHz): δ −68.0 to 83.0 (br, 7F), −100.0 to 135.0 (br, 5F), −138.0 to 144.0 (br, 1F).

Copolymer of lithium perfluoro(4-methyl-3,6-dioxaoct-7-ene) sulfonate and octadecyl vinyl ether (C_{18}-SO_3Li). To synthesize the copolymer **C_{18}-SO_3Li**, a procedure similar to that used for **C_2-SO_3Li** was applied. **C_{18}-SO_3Li** was obtained from **C_{18}-SO_2F** (11.59 g) and Li_2CO_3 (11.50 g, 155.64 mmol) with a 77% yield.

^{1}H-NMR (DMSO-d_6, 400 MHz): δ 4.70–2.00 (br, 5H), 2.00–0.90 (br, 32H), 0.90–0.60 (br, 3H). ^{19}F NMR (DMSO-d_6, 375 MHz): δ −73.0 to 88.0 (br, 7F), −105.0 to 138.0 (br, 5F), −143.0 to 148.0 (br, 1F).

Copolymer of cesium perfluoro(4-methyl-3,6-dioxaoct-7-ene) sulfonate and ethyl vinyl ether (C_2-SO_3Cs). **C_2-SO_2F** (6.45 g), Cs_2CO_3 (12.10 g, 37.14 mmol), and MeOH (200 mL) were placed in a 500 mL two-necked round-bottom flask under a nitrogen atmosphere. The reaction mixture was heated to 50 °C, stirred for 24 h, and then cooled to room temperature. Subsequently, the solution was dialyzed against water to remove the Cs_2CO_3 and CsF. The water was then removed under reduced pressure, affording **C_2-SO_3Cs** with an 86% yield.

^{1}H-NMR (DMSO-d$_6$, 400 MHz): δ 5.00–2.00 (br, 5H), δ 1.60–0.60 (br, 3H). ^{19}F NMR (DMSO-d$_6$, 375 MHz): δ −73.0 to 87.0 (br, 7F), −104.0 to 138.0 (br, 5F), −143.0 to 149.0 (br, 1F).

Copolymer of cesium perfluoro(4-methyl-3,6-dioxaoct-7-ene) sulfonate and butyl vinyl ether (C_4-SO_3Cs). To synthesize the copolymer **C_4-SO_3Cs**, a procedure similar to that used for **C_2-SO_3Cs** was applied. **C_4-SO_3Cs** was obtained from **C_4-SO_2F** (5.47 g) and Cs_2CO_3 (9.80 g, 30.08 mmol) with an 84% yield.

^{1}H-NMR (DMSO-d$_6$, 400 MHz): δ 4.50–2.05 (br, 5H), 1.80–1.10 (br, 4H), 0.95–0.65 (br, 3H). ^{19}F NMR (DMSO-d$_6$, 375 MHz): δ −72.0 to 87.0 (br, 7F), −104.0 to 137.0 (br, 5F), −143.8 to 147.5 (br, 1F).

Copolymer of cesium perfluoro(4-methyl-3,6-dioxaoct-7-ene) sulfonate and dodecyl vinyl ether (C_{12}-SO_3Cs). To synthesize the copolymer **C_{12}-SO_3Cs**, a procedure similar to that used for **C_2-SO_3Cs** was applied. **C_4-SO_3Cs** was obtained from **C_{12}-SO_2F** (10.29 g) and Cs_2CO_3 (15.30 g, 46.96 mmol) with an 88% yield.

^{1}H-NMR (DMSO-d$_6$, 400 MHz): δ 5.35–2.08 (br, 5H), δ 2.00–0.90 (br, 20H), 0.90–0.70 (br, 3H). ^{19}F NMR (DMSO-d$_6$, 375 MHz): δ −72.0 to 87.0 (br, 7F), −105.0 to 133.5 (br, 5F), −142.5 to 147.5 (br, 1F).

Copolymer of cesium perfluoro(4-methyl-3,6-dioxaoct-7-ene) sulfonate and octadecyl vinyl ether (C_{18}-SO_3Cs). To synthesize the copolymer **C_{18}-SO_3Cs**, a procedure similar to that used for **C_2-SO_3Cs** was applied. **C_{18}-SO_3Cs** was obtained from **C_{18}-SO_2F** (9.56 g) and Cs_2CO_3 (12.59 g, 38.64 mmol) with a 93% yield.

^{1}H-NMR (DMSO-d$_6$, 400 MHz): δ 4.80–1.95 (br, 5H), 1.85–0.90 (br, 32H), 0.90–0.70 (br, 3H). ^{19}F NMR (DMSO-d$_6$, 375 MHz): δ −72.0 to 88.0 (br, 7F), −104.0 to 137.0 (br, 5F), −143.0 to 147.5 (br, 1F).

Copolymer of perfluoro(4-methyl-3,6-dioxaoct-7-ene)sulfonic acid and ethyl vinyl ether (C_2-SO_3H). **C_2-SO_3Li** (1.00 g) was dissolved in water (80 mL) in a round-bottom flask. Then, 20 g of concentrated HCl was slowly added to the solution. The mixture was stirred at room temperature for 1 h. After 1 h, the solution was dialyzed against water to remove LiCl and HCl. Finally, the water was removed using a freeze-dryer (FDU-1200), affording **C_2-SO_3H** with a 97% yield.

^{1}H-NMR (DMSO-d$_6$, 400 MHz): δ 5.00–1.80 (br, 5H), δ 1.75–0.65 (br, 3H). ^{19}F NMR (DMSO-d$_6$, 375 MHz): δ −72.0 to 88.0 (br, 7F), −106.0 to 139.0 (br, 5F), −142.5 to 148.0 (br, 1F).

Copolymer of perfluoro(4-methyl-3,6-dioxaoct-7-ene)sulfonic acid and butyl vinyl ether (C_4-SO_3H). To synthesize the copolymer **C_4-SO_3H**, a procedure similar to that used for **C_2-SO_3H** was applied. **C_4-SO_3H** was obtained from **C_4-SO_3Li** (1.00 g) with a 96% yield.

^{1}H-NMR (DMSO-d$_6$, 400 MHz): δ 4.80–2.10 (br, 5H), 1.90–1.10 (br, 4H), 1.00–0.70 (br, 3H). ^{19}F NMR (DMSO-d$_6$, 375 MHz): δ −73.0 to 87.0 (br, 7F), −106.0 to 137.0 (br, 5F), −143.0 to 147.5 (br, 1F).

Copolymer of perfluoro(4-methyl-3,6-dioxaoct-7-ene)sulfonic acid and dodecyl vinyl ether (C_{12}-SO_3H). **C_{12}-SO_3Li** (1.00 g) were dissolved in a mixture of water (40 mL) and MeOH (40 mL) in a round-bottom flask. Then, 20 g of a concentrated HCl solution was slowly added. The resulting mixture was stirred at room temperature for 1 h. After stirring, the solution was dialyzed against water to remove LiCl and HCl. Finally, the water was removed using a freeze-dryer (FDU-1200), affording **C_{12}-SO_3H** with a 96% yield.

^{1}H-NMR (DMSO-d$_6$, 400 MHz): δ 5.95–1.95 (br, 5H), δ 1.90–0.93 (br, 20H), 0.93–0.72 (br, 3H). ^{19}F NMR (DMSO-d$_6$, 375 MHz): δ −71.0 to 88.0 (br, 7F), −106.0 to 140.0 (br, 5F), −143.0 to 148.0 (br, 1F).

Copolymer of perfluoro(4-methyl-3,6-dioxaoct-7-ene)sulfonic acid and octadecyl vinyl ether (C_{18}-SO_3H). To synthesize the copolymer **C18-SO3H**, a procedure similar to that used for **C_{12}-SO_3H** was applied. **C12-SO3H** was obtained from **C18-SO3Li** (1.00 g) with a 97% yield.

^{1}H-NMR (DMSO-d$_6$, 400 MHz): δ 4.85–2.00 (br, 5H), 1.85–0.90 (br, 32H), 0.90–0.65 (br, 3H). ^{19}F-NMR (DMSO-d$_6$, 375 MHz): δ −71.0 to 88.0 (br, 7F), −103.0 to 138.0 (br, 5F), −143.0 to 147.5 (br, 1F).

Results and discussion

Synthesis

Table 1 presents the results of the radical copolymerization of alkyl vinyl ethers **1a–d** with perfluoro(4-methyl-3,6-dioxaoct-7-ene)sulfonyl fluoride **2**. The polymerization proceeded well for all alkyl vinyl ethers. Although the yield was slightly lower with **1a**, this reduction could be attributed to the volatilization of **1a** due to its low boiling point (b.p. 36 °C). The molecular weight

Table 1 Results of radical copolymerization of **1a–d** and **2**[a]

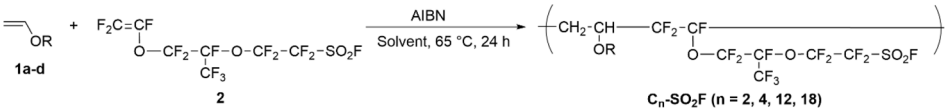

1	R	Solvent	Product	Yield (%)	M_n[b]	PDI[b]
1a	Et	HFC43-10mee	**C_2-SO_2F**	55	593 000	1.5
1b	*n*-Bu	HFC43-10mee	**C_4-SO_2F**	93	254 000	1.8
1c	*n*-$C_{12}H_{25}$	Benzotrifluoride	**C_{12}-SO_2F**	71	153 000	1.4
1d	*n*-$C_{18}H_{37}$	Benzotrifluoride	**C_{18}-SO_2F**	70	145 000	1.4

[a] Conditions: 1 (22.4 mmol), 2 (22.4 mmol), AIBN (0.45 mmol), solvent (10 g). [b] As SO_3Li polymer analyzed by SEC-MALS measurement.

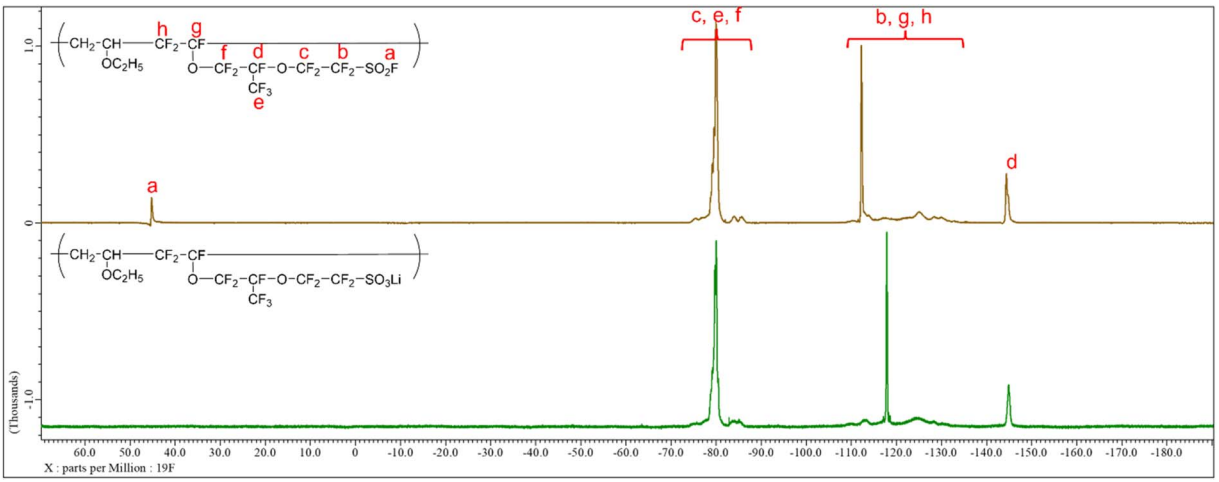

Fig. 2 ^{19}F NMR of C_2-SO_2F (top) and C_2-SO_3Li (bottom).

progressively decreased with longer alkyl chain length, possibly due to steric hindrance inhibiting chain growth and hydrogen abstraction from the hydrocarbon chain terminating propagation. The hydrolysis of the SO_2F moiety in **C_n-SO_2F** was then conducted. Boutevin *et al.* reported that SO_2F can be converted to SO_3Li groups *via* the action of lithium carbonate in methanol on the terpolymer of vinylidene fluoride, chlorotrifluoroethylene, and perfluoro(4-methyl-3,6-dioxaoct-7-ene) sulfonyl fluoride.[25] Following this report, we reacted the sulfonyl fluoride polymer (**C_n-SO_2F**) with lithium carbonate in methanol to obtain the lithium sulfonate polymer (**C_n-SO_3Li**). Fig. 2 shows ^{19}F NMR charts before and after the reaction of **C_2-SO_2F** with Li_2CO_3. Before the reaction, a distinct SO_2F peak (45.2 ppm) was observed in **C_2-SO_2F**. This peak disappeared in **C_2-SO_3Li** after the reaction, while the other peaks remained unchanged, indicating that only the SO_2F group reacted selectively.

Table 2 summarizes the results of the reaction of polymers bearing alkyl ether side chains of different lengths with various carbonates. The reactions proceeded in good yields for the substrates. The corresponding cesium sulfonate polymer (**C_n-SO_3Cs**) was also successfully synthesized using Cs_2CO_3 instead of Li_2CO_3. However, when K_2CO_3 was used, the polymer chains decomposed.

Table 3 lists the calculated and measured elemental analysis results for **C_n-SO_3Li**. The calculated values, based on a 50 : 50 copolymerization ratio of **1 : 2** agreed well with the measured values. The copolymerization ratios of **1** and **2**, determined from the carbon-to-fluorine atomic ratios, were also approximately 50 : 50, indicating successful alternating copolymerization.

The sulfonic acid polymer (**C_n-SO_3H**) was synthesized by adding an excess amount of HCl to **C_n-SO_3Li**, followed by dialysis. Neutralization titration measurements of the ion exchange capacity (IEC) for **C_n-SO_3H** agreed well with the calculated values, indicating that the cation exchange reaction proceeded successfully (Table 4).

Morphology

The morphology of the lithium salt polymer (**C_n-SO_3Li**) in its state was first characterized by SAXS (Fig. 3). All samples exhibited sharp peaks in the 1–8 nm^{-1} range and a broad peak

Table 2 Results of the reaction of C_n-SO_3Cs with carbonate salts

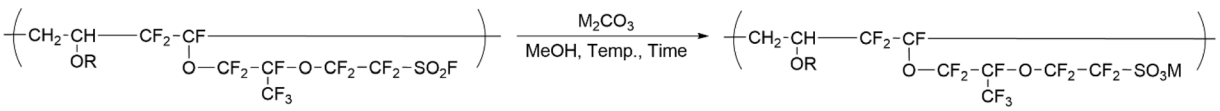

C_n-SO_2F (n = 2, 4, 12, 18) **C_n-SO_3M (n = 2, 4, 12, 18)**

Substrate	R	M	Temp. (°C)	Time (h)	Product	Yield (%)
C_2-SO_2F	Et	Li	65	48	**C_2-SO_3Li**	95
C_2-SO_2F	Et	Cs	50	24	**C_2-SO_3Cs**	86
C_4-SO_2F	*n*-Bu	Li	65	48	**C_4-SO_3Li**	93
C_4-SO_2F	*n*-Bu	Cs	50	24	**C_4-SO_3Cs**	84
C_{12}-SO_2F	*n*-$C_{12}H_{25}$	Li	65	48	**C_{12}-SO_3Li**	91
C_{12}-SO_2F	*n*-$C_{12}H_{25}$	Cs	50	24	**C_{12}-SO_3Cs**	88
C_{18}-SO_2F	*n*-$C_{18}H_{37}$	Li	65	48	**C_{18}-SO_3Li**	77
C_{18}-SO_2F	*n*-$C_{18}H_{37}$	Cs	50	24	**C_{18}-SO_3Cs**	93

Table 3 Calculated and measured values of the elemental analysis of C_n-SO_3Li

Polymer	Elemental analysis								Copolymerization ratio[b]	
	Calcd[a]				Found					
	H [%]	C [%]	F [%]	S [%]	H [%]	C [%]	F [%]	S [%]	1	2
C_2-SO_3Li	1.54	25.40	47.30	6.14	2.20	22.94	45.63	5.44	45	55
C_4-SO_3Li	2.20	28.38	44.90	5.83	2.49	26.48	38.95	4.93	54	46
C_{12}-SO_3Li	4.26	38.08	37.28	4.84	4.13	33.86	35.63	4.51	47	53
C_{18}-SO_3Li	5.40	43.44	33.08	4.29	5.03	40.83	32.14	4.11	49	51

[a] Calculated assuming copolymerization ratio of 50 : 50. [b] calculated from the ratio of C and F elements determined by elemental analysis.

Table 4 Calculated and measured ion exchange group capacity values for C_n-SO_3H

Polymer	Calcd. IEC[a] (meq.)	Found IEC[b] (meq.)
C_2-SO_3H	1.98	1.95
C_4-SO_3H	1.78	1.81
C_{12}-SO_3H	1.58	1.57
C_{18}-SO_3H	1.37	1.32

[a] Calculated from copolymerization ratio. [b] Determined by neutralization titration.

in the 8–16 nm^{-1} range. The sharp peaks correspond to higher-order periodic structures, whereas the broad peak originates from the amorphous halo. Notably, a sharp peak at 15.09 nm^{-1} was observed for **C_{18}-SO_3Li**, which could be attributed to the crystallization of the octadecyl ether side chain.[26] Table 5 lists the peak values for **C_n-SO_3Li** in the 1–8 nm^{-1} region. For all samples, the q value of the n-th peak q_n is n times larger than q_1, suggesting the formation of a lamellar structure. Based on the q values of the first scattering peaks, the d-spacings of (100) diffraction of the lamellar structures of **C_n-SO_3Li** were 2.22 nm ($n = 2$), 2.47 nm ($n = 4$), 3.90 nm ($n = 12$), and 4.62 nm ($n = 18$). These results demonstrate that the d-spacing increased with the elongation of the alkyl ether side chain length. The elongation not only increased the d-spacing but also increased the peak intensity and a greater number of observed peaks (up to the fifth diffraction peak observed in **C_{18}-SO_3Li**). This result indicates an increase in the area of the periodic structure as the side chain lengthen increases.

To observe the morphology in detail, we used TEM. The sample examined was **C_n-SO_3Cs**, which was obtained by reacting **C_n-SO_2F** with cesium carbonate to introduce the heavy metal cesium. The samples were prepared from solid lumps using the ultramicrotome method. The observations revealed that **C_{12}-SO_3Cs** and **C_{18}-SO_3Cs**, with their long alkyl ether side chains, exhibited a striped, periodic structure in the bright-field images (Fig. 4). When we calculated the spacing of the periodic structure from the intensity profile of the Fourier transform image of the bright-field image, the results were consistent with those

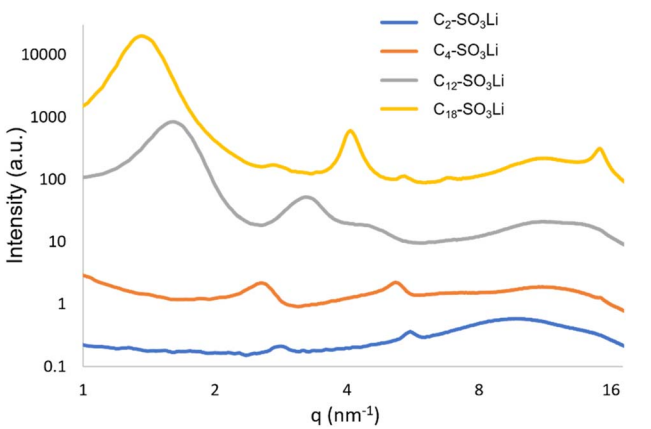

Fig. 3 SAXS profile of C_n-SO_3Li.

Table 5 Peak list in the 1–8 nm^{-1} region and *d*-spacing of (100) diffraction of the SAXS measurements of C_n-SO_3Li

Polymer	q_1 (nm^{-1})	q_2 (nm^{-1})	q_3 (nm^{-1})	q_4 (nm^{-1})	q_5 (nm^{-1})	*d* Spacing of (100) diffraction (nm)
C_2-SO_3Li	2.83	5.58	—	—	—	2.22
C_4-SO_3Li	2.54	5.16	—	—	—	2.47
C_{12}-SO_3Li	1.61	3.22	4–5 (br)	—	—	3.90
C_{18}-SO_3Li	1.36	2.71	4.07	5.40	6.76	4.62

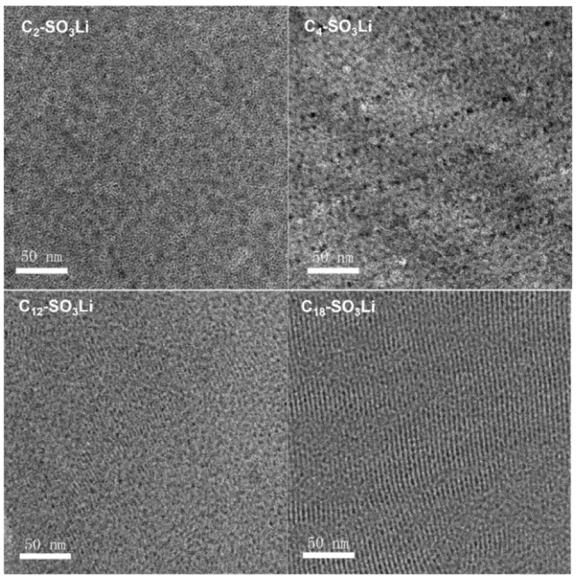

Fig. 4 Bright-field TEM images of C_n-SO_3Cs.

obtained from the SAXS measurements (Fig. S17, S18 and Table 6).

Nafion membranes comprise three phases: (1) uneven hydrophobic domains (tens of nanometers), (2) ion cluster channels (several nanometers), and (3) crystalline phases with interatomic distances (less than one nanometer).[27] In addition, X-ray scattering measurements were performed on Nafion lithium salt membranes, and similar peaks were reported.[28] However, the newly synthesized **C_n-SO_3Li** and **C_n-SO_3Cs** exhibit a completely different morphology. Instead of Nafion-like structures, lamellar structures are formed. Extending the alkyl ether side chain length increases the area of the periodic structure.

In the bright-field TEM images, the dark areas of the periodic structure indicate regions where Cs, which do not transmit electron beams, are present, while the bright areas correspond to areas where Cs are absent. This suggests that the presence of sulfonate groups plays a crucial role in the formation of the structure. In other words, the main chains and alkyl ether side chains of **C_n-SO_3Li** and **C_n-SO_3Cs**, as well as their perfluoroalkyl ether side chains, are hydrophobic, and the sulfonate groups, which are the only hydrophilic moieties, self-assemble to form a lamellar structure (Fig. 5).

In addition, the presence of alkyl ether side chains contributes to the formation of the periodical structures. Poly(alkyl vinyl ethers) with long alkyl side chains are self-assembled because of the intermolecular packing of the side chains.[29–31] Similarly, the long alkyl side chains in **C_n-SO_3Li** and **C_n-SO_3Cs** self-assemble *via* intermolecular alkyl chain packing. In short-chain ethers such as C_2 and C_4, the hydrophobic interactions are weak, leading to relatively low periodicity in their periodic structures. In contrast, in long-chain alkyls, such as C_{12} and C_{18}, these hydrophobic interactions increase. In octadecyl ether, the side-chain portion crystallizes, resulting in higher periodicity.

Self-diffusion coefficiency

Finally, the self-diffusion coefficient of water was measured by pulse field gradient nuclear magnetic resonance (PFG-NMR) spectroscopy of **C_n-SO_3H** (Fig. 6). Surprisingly, the self-diffusion coefficient (*D*) greatly depends on the length of the alkyl vinyl ether chain in the polymer structure. This means that as the alkyl vinyl ether chain length increases, *D* increases, whereas IEC decreases. This inverse relationship between *D* and IEC is due to the improved periodicity of the lamellar structure and the enhanced connectivity of the proton conduction path as the alkyl vinyl ether chain lengthens. In the future, information about designing membranes with high proton conductivity is expected to be obtained by further tuning the molecular structure of the vinyl ether monomers and analyzing their morphology and proton conductivity.

Table 6 Comparison of the *d*-spacing of C_n-SO_3Li and lamellar spacing of C_n-SO_3Cs

Number of alkyl chain	*d* Spacing of **C_n-SO_3Li**[a] (nm)	Lamellar spacing of **C_n-SO_3Cs**[b] (nm)
2	2.22	—
4	2.47	—
12	3.90	3.96
18	4.62	4.82

[a] Determined by SAXS measurement of **C_n-SO_3Li**. [b] Determined by TEM image observation of **C_n-SO_3Cs**.

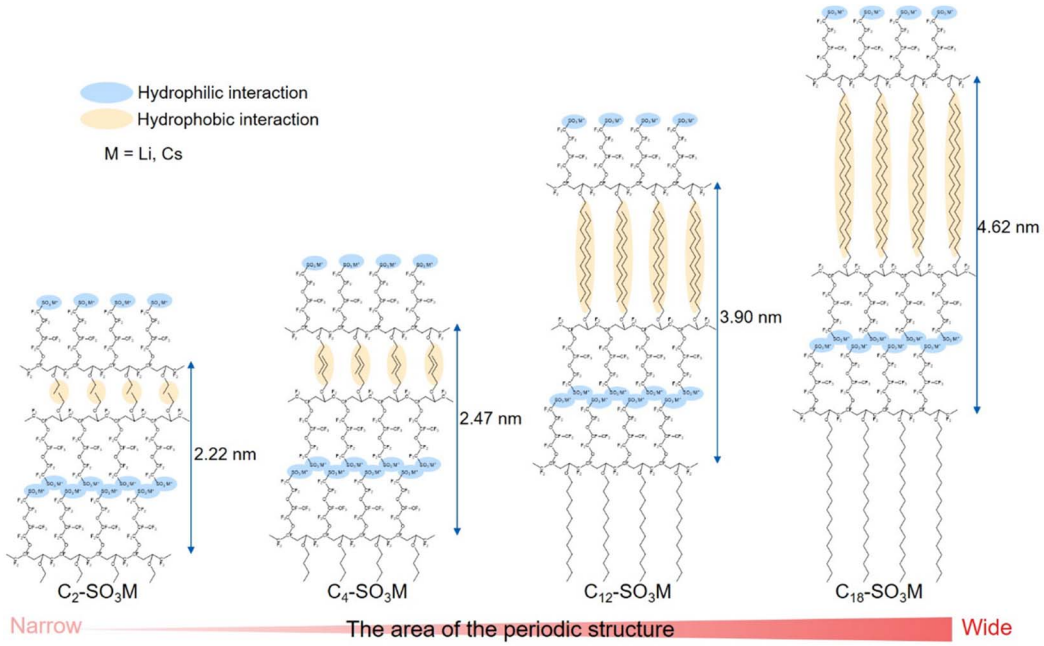

Fig. 5 Schematic illustration of self-assembly.

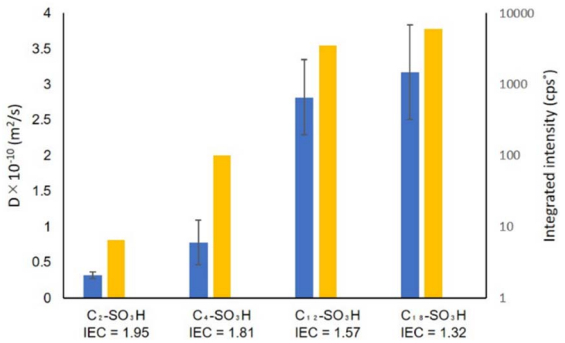

Fig. 6 The self-diffusion coefficient (D) of water in C_n-SO_3H (blue) and the integral intensity of the first peak of C_n-SO_3Li in SAXS (yellow). Error bars were calculated from the 95% confidence interval of the linear fitting.

Conclusions

In this study, a series of alternating copolymers were synthesized by copolymerizing various alkyl vinyl ethers with perfluoro(4-methyl-3,6-dioxaoct-7-ene)sulfonyl fluoride. These copolymers formed lamellar structures. In particular, the copolymer of octadecyl vinyl ether and perfluoro(4-methyl-3,6-dioxaoct-7-ene)sulfonyl fluoride exhibited a lamellar structure over a wide area. Furthermore, the self-diffusion coefficient of water in the polymer increases with increasing alkyl vinyl ether chain length elongates.

Author contributions

All the authors designed the experiments, analysed the data and wrote the paper. K. Hori performed the experiments.

Conflicts of interest

There are no conflicts to declare.

Data availability

The data supporting this article have been included as part of the SI.

Supplementary information file includes NMR spectra, 2D Fourier transfer of TEM bright field image (right) and its strength profile, and PFG-NMR diffusion plot. See DOI: **https://doi.org/10.1039/d5ra04403k**.

Acknowledgements

We thank the TOSOH Analysis and Research Center Co. Ltd for SEC-MALS measurement, Nissan ARC Corp. for TEM image observation and PFG-NMR measurement, and the Core Facility Center at Science Tokyo for SAXS measurement and elemental analysis.

Notes and references

1 S. N. Patel and N. P. Balsara, *Mol. Syst. Des. Eng.*, 2019, **4**, 221.
2 M. A. Morris, H. An, J. L. Lutkenhaus and T. H. Epps, *ACS Energy Lett.*, 2017, **2**, 1919.
3 S. Miyanishi, R. Fukushima and T. Yamaguchi, *Macromolecules*, 2015, **48**, 2576.
4 B. Ghanti and S. Banerjee, *Macromolecules*, 2025, **58**, 3643.
5 P. Patnaik, V. Goyal, S. M. Hossain and U. Chatterjee, *J. Mater. Chem. A*, 2025, **13**, 24971.
6 S. H. Lee, J. Lim, J. Park, M. Kim, Y. Goo and D. Shin, *Int. J. Hydrogen Energy*, 2025, **126**, 459.

7 D. W. Shin, M. D. Guiver and Y. M. Lee, *Chem. Rev.*, 2017, **117**, 4759.
8 J. Peron, Z. Shi and S. Holdcroft, *Energy Environ. Sci.*, 2011, **4**, 1575.
9 M. Rikukawa and K. Sanui, *Prog. Polym. Sci.*, 2000, **25**, 1463.
10 T. D. Gierke, G. E. Munn and F. C. Wilson, *J. Polym. Sci., Polym. Phys. Ed.*, 1981, **19**, 1687.
11 W. Y. Hsu and T. D. Gierke, *J. Membr. Sci.*, 1983, **13**, 307.
12 C. Wang, V. Krishnan, D. Wu, R. Bledsoe, S. J. Paddison and G. Duscher, *J. Mater. Chem. A*, 2013, **1**, 938.
13 G. A. Giffin, G. M. Haugen, S. J. Hamrock and V. D. Noto, *J. Am. Chem. Soc.*, 2013, **135**, 822.
14 Z. Wang, H. Tang, J. Li, Y. Zeng, L. Chen and M. Pan, *J. Power Sources*, 2014, **256**, 383.
15 X. Ling, M. Bonn, S. H. Parekh and K. F. Domke, *Angew. Chem., Int. Ed.*, 2016, **55**, 4011.
16 Z. Long, J. Miyake and K. Miyatake, *Bull. Chem. Soc. Jpn.*, 2020, **93**, 338.
17 T. Mikami, K. Miyatake and M. Watanabe, *ACS Appl. Mater. Interfaces*, 2010, **2**, 1714.
18 R. Tayouo, G. David, B. Améduri, J. Roziére and S. Roualdés, *Macromolecules*, 2010, **43**, 5269.
19 H. Ghassemi, J. E. McGrath and T. A. Zawodzinski, *Polymer*, 2006, **47**, 4132.
20 H.-C. Kim, S.-M. Park and W. Hinsberg, *Chem. Rev.*, 2010, **110**, 146.
21 M. Karayianni and S. Pispas, *J. Polym. Sci.*, 2021, **59**, 1874.
22 M. Ma, X. Guo, P. Wen, S. Han, L. Zhang, Y. Liu, X. Lin and M. Chen, *Angew. Chem., Int. Ed.*, 2024, **63**, e202407304.
23 D. J. Connolly and W. F. Gresham, *US Pat.*, 3282875, 1966.
24 B. H. Thomas, G. Shafer, J. J. Ma, M.-H. Tu and D. D DesMarteau, *J. Fluorine Chem.*, 2004, **125**, 1231.
25 L. Saugiet, B. Ameduri and B. Boutevin, *J. Polym. Sci., Part A: Polym. Chem.*, 2007, **45**, 1814.
26 J. Li, H. Wang, L. Kong, Y. Zhou, S. Li and H. Shi, *Macromolecules*, 2018, **51**, 8922.
27 S. P. F. Bordín, H. E. Andrada, A. C. Carreras, G. E. Castellano, R. G. Oliveira and V. M. G. Josa, *Polymer*, 2018, **155**, 58.
28 L. Mazzapioda, F. Piccolo, A. D. Giudice, L. Silvestri and M. A. Navarra, *Materials for Renewable and Sustainable Energy*, 2024, **13**, 59.
29 X. Zhang, W. Reyntjens and E. J. Goethals, *Polym. Int.*, 2000, **49**, 277.
30 T. Yoshida, K. Seno, S. Kanaoka and S. Aoshima, *J. Polym. Sci., Part A: Polym. Chem.*, 2005, **43**, 1155.
31 T. Yoshida, S. Kanaoka, H. Watanabe and S. Aoshima, *J. Polym. Sci., Part A: Polym. Chem.*, 2005, **43**, 2712.